

β,β -Carotene Decreases Peroxisome Proliferator Receptor γ Activity and Reduces Lipid Storage Capacity of Adipocytes in a β,β -Carotene Oxygenase 1-dependent Manner^{*[5]}

Received for publication, April 9, 2010, and in revised form, June 2, 2010. Published, JBC Papers in Press, June 23, 2010, DOI 10.1074/jbc.M110.132571

Glenn P. Lobo[‡], Jaume Amengual[‡], Hua Nan M. Li[‡], Marcin Golczak[‡], M. Luisa Bonet[§], Krzysztof Palczewski[‡], and Johannes von Lintig^{‡1}

From the [‡]Department of Pharmacology, School of Medicine, Case Western Reserve University, Cleveland, Ohio 44106 and the [§]Laboratory of Molecular Biology, Nutrition and Biotechnology, Universitat de les Illes Balears and CIBERobn, 07122 Palma de Mallorca, Spain

Increasing evidence has been provided for a connection between retinoid metabolism and the activity of peroxisome proliferator receptors (Ppars) in the control of body fat reserves. Two different precursors for retinoids exist in the diet as preformed vitamin A (all-*trans*-retinol) and provitamin A (β,β -carotene). For retinoid production, β,β -carotene is converted to retinaldehyde by β,β -carotene monooxygenase 1 (Bcmo1). Previous analysis showed that *Bcmo1* knock-out mice develop dyslipidemia and are more susceptible to diet-induced obesity. However, the role of *Bcmo1* for adipocyte retinoid metabolism has yet not been well defined. Here, we showed that *Bcmo1* mRNA and protein expression are induced during adipogenesis in NIH 3T3-L1 cells. In mature adipocytes, β,β -carotene but not all-*trans*-retinol was metabolized to retinoic acid (RA). RA decreased the expression of Ppar γ and CCAAT/enhancer-binding protein α , key lipogenic transcription factors, and reduced the lipid content of mature adipocytes. This process was inhibited by the retinoic acid receptor antagonist LE450, showing that it involves canonical retinoid signaling. Accordingly, gavage of β,β -carotene but not all-*trans*-retinol induced retinoid signaling and decreased Ppar γ expression in white adipose tissue of vitamin A-deficient mice. Our study identifies β,β -carotene as a critical physiological precursor for RA production in adipocytes and implicates provitamin A as a dietary regulator of body fat reserves.

Among the many functions attributed to retinoids, its putative role in adipocyte biology and the regulation of body fat reserves have generated clinical and scientific interest (reviewed in Refs. 1, 2). Animal studies indicate that diets low in vitamin A favor adipose tissue formation (3, 4) and enhance formation of intramuscular fat (5). Regulation of fat reserves by dietary vitamin A can be explained by the metabolism of vitamin A to biologically active retinoid derivatives, which then impact the differentiation and function of adipose tissue. The

vitamin A derivative all-*trans*-retinoic acid (RA)² has been shown to inhibit adipocyte differentiation in cell culture (6, 7). In mature adipocytes, treatment with pharmacological doses of RA can induce lipolysis (4, 8), mitochondrial uncoupling (9, 10), and oxidative metabolism (11, 12) and influence the production of adipokines (13–16) both in cell culture and mouse models. Many of these effects are likely mediated by retinoic acid receptors (Rars). Rars are transcription factors that act in conjunction with retinoid X receptors (Rxrs) (17) to regulate the expression of numerous target genes in response to RA binding. Additionally, some effects of RA appear to arise from the activation of Ppar β and $-\delta$ (8). Furthermore, the RA precursor retinaldehyde is present in fat *in vivo* and can inhibit Ppar γ -induced adipogenesis (18).

A prerequisite for the initiation of vitamin A-dependent physiological processes is the production of these biologically active retinoids from dietary precursors. Surprisingly, high dose supplementation with preformed vitamin A does not affect body adiposity in mice (19). Hence, it is yet not clear whether dietary vitamin A can influence physiological energy balance and fat storage. Besides preformed vitamin A, β,β -carotene (BC) is a dietary source for retinoids. BC is oxidatively converted to RAL by the action of BC monooxygenase 1 (*Bcmo1*), an enzyme expressed in various tissues, including the intestine, liver, and adipocytes (20–22). *Bcmo1* gene transcription is under the control of Ppar γ (23, 24), a key regulator of adipocyte differentiation and lipogenesis in mature adipocytes (reviewed in Ref. 25). However, the roles and relationships of *Bcmo1* and Ppar γ in adipocyte biology and the regulation of fat reserves have yet to be further advanced.

Recent studies in knock-out mice indicate that *Bcmo1* is the key enzyme for vitamin A production (26, 27). Aside from grossly impaired BC metabolism, this mouse mutant develops dyslipidemia, is more susceptible to diet-induced obesity, and shows increased expression of Ppar γ -induced genes in adipocytes (26). Importantly, these abnormalities were noted in *Bcmo1*-deficient mice well supplied with vitamin A, indicating

* This work was supported, in whole or in part, by National Institutes of Health Grants EY019641, EY009339, and T30-EY11373.

[5] The on-line version of this article (available at <http://www.jbc.org>) contains supplemental Figs. S1–S4.

¹ To whom correspondence may be addressed: Dept. of Pharmacology (W333), Case Western Reserve University, 10900 Euclid Ave., Cleveland, OH 44160. Tel.: 216-368-3528; Fax: 216-368-1300; E-mail: Johannes.vonlintig@case.edu.

² The abbreviations used are: RA, all-*trans*-retinoic acid; BC, β,β -carotene; C/Ebp α , CCAAT/enhancer-binding protein α ; FHR, fenretinide; iWAT, inguinal white adipose tissue; Ppar, peroxisome proliferator-activated receptor; RAL, all-*trans*-retinal; Rar, retinoic acid receptor; Rxr, retinoid X receptor; ROL, all-*trans*-retinol; RE, retinyl esters; TG, triacylglycerol; VAD, vitamin A-deficient diet; qRT-PCR, quantitative RT-PCR.

Bcml1 and Adipocyte Biology

an important role of Bcml1 for the regulation of lipid metabolism. Here, we here analyzed the role of Bcml1 for retinoid metabolism of adipocytes by using both the NIH 3T3-L1 adipocyte cell culture system and mouse models.

EXPERIMENTAL PROCEDURES

Materials—All chemicals, unless stated otherwise, were purchased from Sigma. All reagents for cDNA synthesis and quantitative real time PCR (qRT-PCR) were purchased from Applied BioSystems (Foster City, CA). Dulbecco's modified Eagle's medium (DMEM) and fetal bovine serum (FBS) were obtained from Invitrogen. The M-PER mammalian protein isolation reagent, BCA, Bradford protein assay kits, and the ECL reagents were purchased from Pierce. The triacylglycerol assay kit (catalog no. TG-1-NC) was purchased from Zen Bio (Research Triangle Park, NC). Primary antibodies against PPAR γ and Fabp4/aP2 were obtained from Cell Signaling Technologies (Beverly, MA). Primary antibody against Ras-regulated nuclear protein (Ran) was purchased from Abcam (Cambridge, MA). The anti-mouse and anti-rabbit horseradish peroxidase-conjugated secondary antibodies were purchased from Promega (Madison, WI).

Cell Culture—Mouse preadipocyte NIH 3T3-L1 cells were maintained in DMEM supplemented with 10% fetal bovine serum (FBS) and 1% penicillin/streptomycin sulfate and cultured at 37 °C in 5% CO₂. To induce differentiation, 2 days after reaching confluence (day 0), cells were placed in differentiation media consisting of DMEM, 10% serum, 0.5 mM 3-isobutyl-1-methylxanthine, 10 μ g/ml insulin, and 0.25 mM dexamethasone for 3 days. On day 3, cells were incubated with DMEM containing 10% serum and 10 μ g/ml insulin for 2 more days. Medium was then replaced with fresh DMEM containing 10% FBS, and cells were allowed to differentiate further. Stock solutions of BC, all-*trans*-retinol (ROL), and citral were prepared in appropriate reagents as suggested by the manufacturer (Sigma). BC was from Wild (Germany), and fenretinide was from Toronto Research Chemicals (Ontario, Canada). With the exception of citral (10 μ M), all other metabolites were prepared at a final concentration of 2 μ M in tetrahydrofuran (THF) for delivery to cells. Final concentrations of the solvent in cell culture media were always 0.1% (v/v). Control cells were treated with complete medium containing 0.1% THF (v/v). For experimental treatments, the appropriate metabolite was added to mature NIH 3T3-L1 cells in THF on day 5. Treated cells then were incubated for 24 h before harvesting. Harvested cells were either processed immediately for RNA, protein, or HPLC analyses or frozen at -80 °C until needed. For the RAR pan-antagonist LE540 experiment, mature NIH 3T3-L1 cells were pretreated with 1 μ M of LE540 for 1 h prior to addition of BC (2 μ M), and cells were incubated for an additional 24 h. After harvesting, cells were processed for total RNA. mRNA expression of relevant genes was determined by quantitative real time-PCR (qRT-PCR) with gene-specific probe sets (Applied BioSystems).

RNA Isolation and Quantitative Real Time PCR Analysis—RNA was isolated from mouse adipose tissue or cultured adipocytes (\pm indicated treatments) with the TRIzol reagent (Invitrogen), purified by using the RNeasy system (Qiagen),

and then quantified spectrophotometrically, as described previously (28). About 2 μ g of total RNA was reverse-transcribed by using the High Capacity RNA-to-cDNA kit and following the manufacturer's instructions (Applied BioSystems). q-PCR was carried out with TaqMan chemistry, namely TaqMan Gene Expression Master Mix and Assays on Demand probes (Applied BioSystems) for mouse *Ppar γ* (Mm01184323_m1), mouse *Bcml1* (Mm00502437_m1), mouse *Fabp4/aP2* (Mm0044588_m1), mouse *C/Ebpa* (Mm00514283_s1), mouse *Cyp26a1* (Mm00514486_m1), mouse *Raldh1* (Mm00657317_m1), and mouse *Adh1* (Mm00507711_m1). The 18 S rRNA (4319413E) probe set (Applied BioSystems) was used as the endogenous control. All real time experiments were done with the Applied BioSystems Step-One Plus qRT-PCR machine. To control for between-sample variability, mRNA levels were normalized to 18 S rRNA for each sample by subtracting the *Ct* for 18 S rRNA from the *Ct* for the gene of interest, thereby producing a ΔCt value. The ΔCt for each treatment sample was compared with the mean ΔCt for control samples by using the relative quantitation $2^{-(\Delta\Delta Ct)}$ method to determine fold-changes (Applied BioSystems Technical Bulletin No. 2).

Semi-quantitative PCR—Total RNA was isolated from control or experimental NIH 3T3-L1 cells, and first-strand cDNA synthesis was achieved by using the High Capacity RNA-to-cDNA kit following the manufacturer's instructions (Applied BioSystems). Semi-quantitative PCR was performed with primers as follows: mouse *Fabp4/aP2* (adipocyte lipid-binding protein), 5'-GAACCTGGAAGCTTGTCTTCG-3' and 5'-ACCAGCTTGTCCACCATCTCG-3'; mouse *Bcml1*, 5'-TGTTTCTGGAGCAGCCTTTT-3' and 5'-CGTAGGCATTGACATGATGG-3'; mouse retinol saturase, 5'-TGCCAGATGTGAAGAAGCAG-3' and 5'-GAAGGGGAATGTGTTCTGGA-3'; and mouse cyclophilin (*Cyc*) 5'-TCCAAAGACAGCAGAAAACCTTTCG-3' and 5'-TCTTCTTGCTGGTCTTGC-CATTCC-3'. The PCR program included denaturation at 94 °C for 30 s, annealing at 55 °C for 30 s, and elongation at 72 °C for 60 s (for a total of 25 cycles). PCR products were separated by electrophoresis on 2% (w/v) agarose gels.

Immunoblotting Analyses—Total protein from mouse adipose tissue or cultured cells was isolated as described previously (28) at indicated time points by using the M-PER mammalian protein extraction reagent with protease inhibitors (Roche Applied Science) according to the manufacturer's instructions (Pierce). Mice were sacrificed by cervical dislocation. Appropriate adipose tissues were collected, rinsed in ice-cold phosphate-buffered saline (PBS) (pH 7.4), and snap-frozen in liquid nitrogen. Mouse adipose tissue (~100 mg) was then homogenized in liquid nitrogen with a mortar and pestle and transferred directly into M-PER buffer (500 μ l) containing protease inhibitors and further processed as outlined by the manufacturer (Pierce). Samples were centrifuged at 12,000 rpm for 15 min at 4 °C, and protein content in the supernatant was determined by using either the bicinchoninic acid assay (BCA) reagent (Pierce) or the Bradford assay (Bio-Rad). Proteins (30–50 μ g) were fractionated on 4–10% SDS-polyacrylamide gels with the Bio-Rad mini-gel system and transferred onto polyvinylidene fluoride (PVDF) membranes (Millipore). Equal protein loading was

confirmed by Ponceau S staining and by immunoblotting analysis with anti-Ran. PVDF membranes were blocked by either 5% milk prepared in Tris/HCl (pH 7.4) and 100 mM NaCl, containing 0.05% Tween (TBS-T) or Super-block (Pierce) for 2–4 h and then immunoblotted with either anti-Ppar γ , anti-FABP4/aP2, anti-Bcmo1 (1:1000 dilution), or anti-RAN antibody (1:5000 dilution) overnight at 4 °C. After multiple washes with TBS-T, membranes were then incubated with the appropriate horseradish peroxidase-conjugated secondary antibody for 1 h at room temperature before being visualized with the ECL detection system (Pierce).

Quantitative Analysis of Immunoblotting Data—Measurements of signal intensity on PVDF membranes after immunoblotting with various antibodies were performed by using an AlphaImager densitometer with the AlphaEaseFC image processing and analysis software (Alpha Innotech). For statistical analyses, all data were expressed as integrated density values, which were calculated as the density values of specific protein bands/RAN density values and expressed as percentages of the control. All figures showing quantitative analyses include data obtained from at least three independent experiments.

Oil Red-O Staining—Cells were washed twice with PBS, fixed with 4% paraformaldehyde for a minimum of 1 h at room temperature, and then stained for 2 h with Oil Red-O solution (0.5% Oil Red-O in 100% isopropyl alcohol). After staining, cells were washed twice with PBS and visualized with an inverted microscope. Quantification of Oil Red-O stain from stained cells was performed by eluting the stain from cells with 1 ml of 100% isopropyl alcohol and then measuring the absorbance of the stain against a blank (100% isopropyl alcohol at 500 nm). This experiment was repeated three times and performed with at least four replicates per treatment.

Triacylglycerol Accumulation Assay—To determine the extent of lipid accumulation of experimental cells as compared with controls, we made use of the TG assay kit (Zen-Bio) and followed the manufacturer's instructions. The reagent allows measurement of the concentration of glycerol released after lysing the cells and hydrolyzing the TG molecules. The TG concentration can then be determined from the glycerol values. For this experiment, mature adipocytes were treated with either 0.1% THF (vehicle control) or test compounds for 24 h, and the free glycerol released was assayed by using the TG assay kit for NIH 3T3-L1 adipocytes (Zen-Bio) and following the manufacturer's instructions. The experiment was repeated twice with at least four replicates for each condition.

Extraction of BC and Retinoids for HPLC and LC/MS Analysis—Retinoids and carotenoids were extracted from serum under a dim red safety light (600 nm) as described previously (26). Adipose tissue (~40 mg) was incubated with 100 μ l of 12% pyrogallol in ethanol, 200 μ l of 30% KOH in water, and 1 ml of ethanol for 2 h at 37 °C. After saponification, 1 ml of H₂O was added. Retinoids were extracted twice with 3 ml of ether/hexane (2:1, stabilized with 1% ethanol) and diluted with 2 ml of H₂O and 2 ml ethanol. After centrifugation for 5 min at 800 \times g, the organic layer was collected. The extract was evaporated in a SpeedVac, and the residue was dissolved in HPLC solvent. For extraction of nonpolar and polar retinoids, 25 mg of NIH 3T3-L1 cells were homogenized in 200 μ l of 2 M hydrox-

ylamine (pH 6.8) and 400 μ l of methanol. After 10 min, 10 μ l of 5 M KOH were added. Nonpolar retinoids were extracted with 750 μ l of hexane, and the organic phase was collected. Then 600 μ l of 4 N HCl and 30 μ l of saturated NaCl solution were added to the aqueous phase. After acidification, polar retinoids were extracted with 750 μ l of hexane. Organic phases were dried in a SpeedVac. Polar retinoids were dissolved in HPLC solvent 1 (81% hexane, 19% ethyl acetate, 12.5 μ l of acetic acid per 100 ml), and nonpolar retinoids and BC were dissolved in HPLC solvent 2 (99.5% hexane and 0.5% ethanol). HPLC separation of BC and different retinoids and quantification of peak integrals were performed as described previously (29, 30). The identity of retinoic acid was further confirmed by LC/MS. The polar retinoid extract was injected onto a Zorbax Sil column (Agilent Technologies, Santa Clara, CA) equilibrated with 81% hexane, 19% ethyl acetate, and 12.5 μ l of acetic acid per 100 ml. The eluant was directed into LXQ mass spectrometer through an atmospheric pressure chemical ionization source (Thermo Scientific, Waltham, MA) working in a positive mode. Retinoic acid was identified based on its molecular mass ($m/z = 301$ [MH]⁺) and a fragmentation pattern of the parent ion identical with that of a synthetic standard (Sigma).

Enzymatic Assays—Recombinant Bcmo1 was expressed in *Escherichia coli*. Protein preparation and tests for enzymatic activity were conducted as described previously (31). Fenretinide (FHR) was purchased from Toronto Research Chemical (Toronto, Canada) and was dissolved in ethanol and delivered together with the BC substrate in *n*-octyl- β -D-thioglucopyranoside micelles (3% w/v).

Animals and Diets—Animal experiments were performed in accordance with United States animal protection laws by the guidelines of the local veterinary authorities. The lecithin-retinoid acyltransferase-deficient mice (*Lrat*^{-/-}) were kept in a room with controlled conditions (24 °C, 12:12-h light/dark cycle) with free access to food and water. In the first experiment, 8-week-old *Lrat*^{-/-} mice ($n = 5$ animals per group) were fed for 3 weeks with a vitamin A-sufficient diet, containing 15,000 IU/kg or vitamin A-deficient diet (VAD) (AIN-93G Growing Rodent Diet With or without Added vitamin A; Research Diets, New Brunswick, NJ). After this period, animals were sacrificed, and the liver and inguinal white adipose tissues (iWAT) were excised in their entirety, weighed, snap-frozen in liquid nitrogen, and stored at -80 °C until analysis. To analyze the effects of BC on iWAT, *Lrat*^{-/-} mice were fed for 10 days with the VAD diet based on a AIN-93G formulation (Research Diets, New Brunswick, NJ). HPLC analysis revealed that BC was below detection levels in this diet (data not shown). After this period, animals ($n = 3$ per group) were gavaged one time with 0.5 mg of BC (DSM Nutritional Products, Sisseln, Switzerland) or 0.5 mg of ROL (Sigma) dissolved in 100 μ l of corn oil. As control, animals were gavaged with vehicle only. After 24 h, animals were sacrificed, and the liver and iWAT were removed, snap-frozen in liquid nitrogen, and stored at -80 °C until further analyses. In an additional experiment, *Lrat*^{-/-} mice were fed for 10 days with the VAD diet. The animals ($n = 5$ per group) were gavaged three times, 24 h apart, with 0.5 mg of BC (DSM Nutritional Products, Sisseln, Switzerland) or 0.5 mg of ROL (Sigma) dissolved in 100 μ l of corn oil. After 24 h, animals

Bcmo1 and Adipocyte Biology

were sacrificed, and the liver and iWAT were removed, snap-frozen in liquid nitrogen, and stored at -80°C until further analyses. In all experiments, animals had free access to water and food and were sacrificed in the fed state.

H&E Staining of Mouse Adipose Tissue—Mouse adipose tissues were fixed in neutral buffered formalin for 24 h and processed routinely into paraffin blocks, and representative histological sections (10 μm) of each specimen were stained with hematoxylin and eosin (Merck) according to the described standard staining protocol being used at the Histology Core Facility (Institute of Pathology, Visual Sciences Research Center, University Hospitals, Cleveland, OH). Images were collected through an Olympus BX 60 microscope equipped with a $\times 20$ objective and a SPOT camera (Diagnostic Instruments, Sterling Heights, MI). Adipocyte images then were analyzed with Metamorph Imaging Software (Molecular Devices, Downingtown, PA). Approximately 600 individual adipocytes were sized per condition. Average areas of adipocytes are expressed in square microns.

Statistical Analyses—Results are presented as means \pm S.D., and the number of experiments is indicated in the figure legends. For each experiment, all determinations were performed at least in triplicate. Statistical significance was assessed by using the two-tailed Student's *t* test.

RESULTS

Bcmo1 Expression Is Induced during Adipocyte Differentiation—The murine *Bcmo1* promoter contains a DR1-type peroxisome proliferator-response element (supplemental Fig. S1A) that binds Ppar γ /R α heterodimers (23), prompting us to examine expression patterns of *Bcmo1* during adipocyte differentiation in the well established mouse NIH 3T3-L1 adipocyte cell culture model. Adipocyte differentiation was monitored by using Oil Red-O staining to assess lipid accumulation (supplemental Fig. S1B) and by following the mRNA expression of adipose marker genes, *i.e.* Ppar γ , fatty acid-binding protein 4 (*FabP4/aP2*), and retinol saturase (*RetSat*). Semi-quantitative PCR analysis revealed that *Bcmo1* mRNA expression increased during adipocyte differentiation and achieved maximal levels in mature NIH 3T3-L1 adipocytes (Fig. 1A). qRT-PCR analysis confirmed that *Bcmo1* mRNA levels were 5-fold elevated in mature adipocytes as compared with preadipocytes (supplemental Fig. S1C). Immunoblotting revealed a 7-fold increase of *Bcmo1* at the protein level upon adipocyte differentiation (Fig. 1B and supplemental Fig. S1D). Thus, as expected for a Ppar γ -inducible target gene, *Bcmo1* expression increased during adipocyte differentiation at both the mRNA and protein levels.

BC but Not ROL Decreases Lipid Content of Mature Adipocytes—We next tested whether the *Bcmo1* substrate BC can impact adipocyte biology by treating mature NIH 3T3-L1 adipocytes with either 2.0 μM BC or vehicle alone (control cells). Additionally, cells were treated with 2 μM ROL, the other circulating precursor of biologically active retinoids. After 24 h, cells were fixed, and Oil Red-O staining for lipids was performed. BC-treated cells showed less staining for lipids compared with ROL-treated and control cells (Fig. 1C). Microscopic inspection revealed that lipid droplets were reduced in

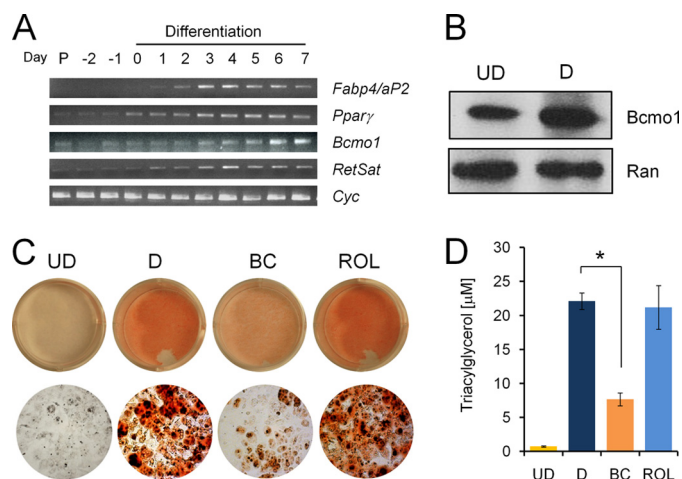


FIGURE 1. Induction of *Bcmo1* expression during adipogenesis. NIH 3T3-L1 mouse preadipocytes were induced to differentiate into mature adipocytes as outlined under "Experimental Procedures." Day 0 represents 2 days post-confluence and the starting point of the differentiation program. **A**, semi-quantitative RT-PCR analysis of mRNA expression of marker genes for adipogenesis (*Fabp4/aP2*, *Ppar γ* , and retinol saturase (*RetSat*)), *Bcmo1*, and cyclophilin (*Cyc*, used as loading control). Shown are PCR products after electrophoresis on 2% (w/v) ethidium bromide-agarose gels. **P**, parental undifferentiated preadipocytes. **B**, representative immunoblots showing expression of *Bcmo1* protein. **UD**, undifferentiated preadipocytes; **D**, differentiated adipocytes at day 5. **C**, Oil Red-O staining of undifferentiated preadipocytes and differentiated adipocytes at day 5 treated with vehicle only and BC or ROL, respectively. **Top panels** show representative images of cells stained with Oil Red-O; **bottom panel** are images from Oil Red-O-stained cells taken at $\times 20$ magnification. **D**, TG content of NIH 3T3-L1 cells treated as indicated. Error bars represent S.D., $n = 3$ per condition; two-tailed Student's *t* test; *, $p < 0.001$.

size and number in BC-treated compared with control or ROL-treated cells (Fig. 1C, bottom panel). Spectrophotometric quantification indicated that BC-treated cells displayed a 2.8-fold reduced staining with Oil Red-O compared with nontreated and ROL-treated cells (supplemental Fig. S1E). Likewise, the triacylglycerol (TG) content of adipocytes was 2.7-fold reduced upon BC but not ROL treatment of these differentiated cells (Fig. 1D).

fenretinide Selectively Inhibits BC Effects on Adipocytes—Our study showed that BC can reduce TG content in mature NIH 3T3-L1 adipocytes. To discriminate between the effects of parent BC and its retinoid derivatives, we needed a highly selective inhibitor of *Bcmo1* enzymatic activity. Positively charged retinoids such as retinylamine selectively block the activity of the retinoid isomerase Rpe65 (32) that is structurally related to *Bcmo1*. Retinylamine can be converted to retinylamides (33), and aromatic amide conjugates have recently been shown to inhibit the activity of related plant carotenoid oxygenases (34). A compound that combines the chemical properties of retinylamine and aromatic amides is FHR. To test whether FHR inhibits *Bcmo1* activity, we expressed murine *Bcmo1* in *E. coli* and delivered BC in *n*-octyl- β -D-thioglucopyranoside micelles. Recombinant *Bcmo1* metabolized BC to RAL, and the reaction was linear for 10 min (Fig. 2A). We then delivered BC in *n*-octyl- β -D-thioglucopyranoside micelles in the presence of increasing amounts of FHR. As shown in Fig. 2B, FHR inhibited the activity of recombinant *Bcmo1* in a dose-dependent manner. So we then treated mature NIH 3T3-L1 adipocytes with BC in the absence and presence of FHR. After 24 h, we stained cells with

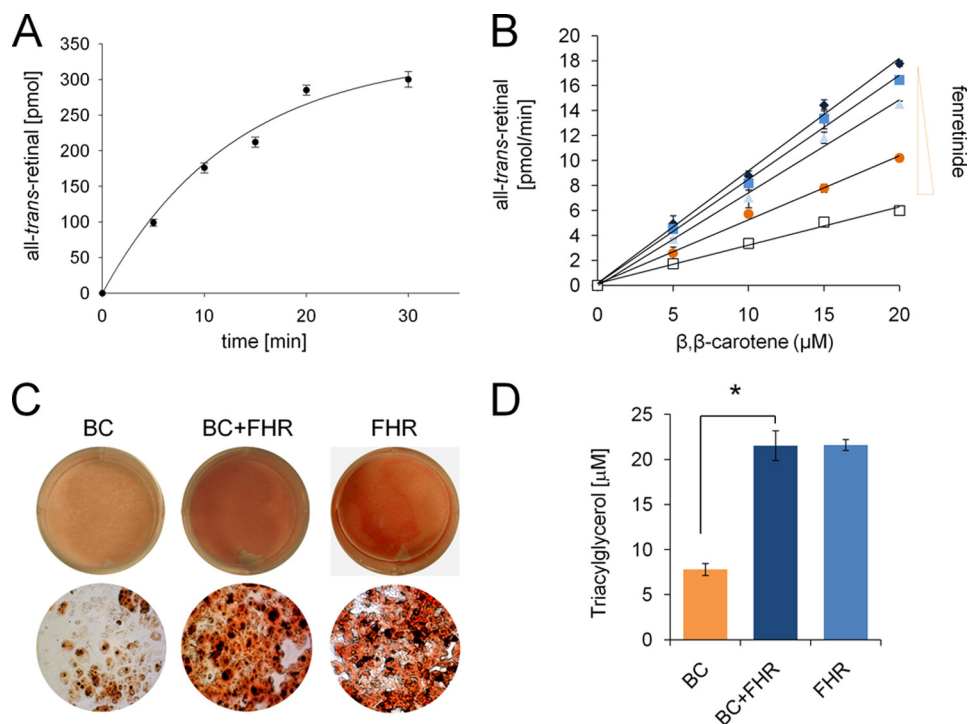


FIGURE 2. Fenretinide selectively inhibits the anti-adipogenic effects of β, β -carotene. *A*, recombinant murine Bcmo1 was incubated with β, β -carotene ($20 \mu\text{M}$) for different time intervals. *B*, recombinant murine Bcmo1 was incubated in the presence of increasing concentrations of BC in the absence and presence of increasing amounts of FHR. Reactions were run for 10 min at 28°C . In the graph, product formation is plotted against the substrate concentration. *Diamonds*, no FHR; *squares*, $0.1 \mu\text{M}$ FHR; *triangles*, $0.3 \mu\text{M}$ FHR; *circles*, $0.9 \mu\text{M}$ FHR; *open squares*, $2.0 \mu\text{M}$ FHR. *C*, Oil Red-O staining of mature NIH 3T3-L1 cells treated with $2 \mu\text{M}$ BC in the presence and absence of $2 \mu\text{M}$ fenretinide. As control, cells were treated with $2 \mu\text{M}$ fenretinide only. *D*, TG content of NIH 3T3-L1 cells. Error bars represent S.D., $n = 3$ per condition; two-tailed Student's *t* test; *, $p < 0.001$.

Oil Red-O for lipids (Fig. 2*C*) and measured cellular TG content (Fig. 2*D*). Although BC treatment alone reduced TG content, this effect was largely prevented by FHR. Treatment with FHR only did not result in a reduction of TG content (Fig. 2*D*). Thus, FHR selectively inhibited the effects of BC on adipocyte lipid content, indicating that they are dependent on Bcmo1 activity.

BC but Not ROL Is Converted to RA in Mature Adipocytes—To determine the biologically active retinoid derivative that mediates this effect, we extracted nonpolar and polar retinoids and performed HPLC analyses. In BC-treated adipocytes, no increase of ROL and/or retinyl ester (RE) levels was found (Fig. 3*A*), but these cells produced RA ($9.6 \pm 2 \text{ pmol/mg}$) (Fig. 3*A*), the identity of which was confirmed by tandem mass spectrometry [$\text{MH}]^+ = 301$ and [$\text{MH} - \text{H}_2\text{O}]^+ = 283$ (Fig. 3, *C* and *D*). Treatment of adipocytes with BC in the presence of the Bcmo1 inhibitor FHR reduced the production of RA by 8-fold ($1.2 \pm 0.42 \text{ pmol/mg}$) (Fig. 3*A*). In ROL-treated adipocytes, a strong increase in RE and ROL levels was detected, but RA was below the detection limit (Fig. 3*B*). Thus, BC and ROL have different metabolic fates in NIH 3T3-L1 adipocytes, being metabolized to RA and RE, respectively.

BC Represses Ppar γ and CCAAT/Enhancer-binding Protein α Expression in Mature Adipocytes—RA treatment inhibits adipose conversion of preadipocyte cell lines by reducing the expression of the key lipogenic transcription factors CCAAT/enhancer-binding protein α (C/EBP α) and Ppar γ (7). However, these transcription factors are less responsive to RA in mature

NIH3T3-L1 adipocytes (16, 35). No reduction of the lipid content of mature NIH 3T3-L1 adipocytes was found treated with 0.5 and $10 \mu\text{M}$ of RA, respectively (supplemental Fig. S2). In contrast, treatment with 0.5 and $2 \mu\text{M}$ BC significantly decreased lipid content (supplemental Fig. S2). Ppar γ and C/EBP α mRNA levels were 3.1- and 2.4-fold reduced, respectively, in mature NIH 3T3-L1 adipocytes treated with BC as compared with control and ROL- or RA-treated mature adipocytes (Fig. 4, *A* and *B*). The decreased Ppar γ mRNA levels were paralleled by 3.6-fold reduction of Ppar γ protein levels as evidenced by immunoblot analysis (Fig. 4, *D* and *E*). The down-regulatory effects of BC on Ppar γ and C/EBP α expression were prevented by co-treatment with FHR, which inhibited Bcmo1 activity (Fig. 4). To explain the discrepancy between the effects in our cell system of exogenously applied RA and endogenous RA synthesized from BC, we performed HPLC analysis. This analysis showed that cellular RA levels were 12-fold lower after treatment with $2 \mu\text{M}$ exogenous RA ($0.8 \pm 0.38 \text{ pmol/mg}$) than in $2 \mu\text{M}$ BC-treated ($9.6 \pm 2 \text{ pmol/mg}$) mature NIH 3T3 cells (Fig. 3*A*). Measurement of the pH of the medium of preadipocytes and mature adipocytes, being 7.3 and 8.1, respectively, gave an explanation for differences in RA sensitivity. Considering the pK_a value of RA being ~ 6 (37), the conjugated base exists in ~ 10 -fold higher amounts at pH 8.1 as compared with pH 7.3, and this negatively charged compound cannot easily enter cells by passive diffusion. We also exclude that effects of BC are mediated by the primary cleavage product RAL that recently was shown to inhibit Ppar γ activity and to repress adipocyte differentiation (18). Treatment of cells with BC in the presence of citral, an inhibitor of retinal dehydrogenases (Raldhs), did not reproduce the inhibitory effects of treatment with BC alone on Ppar γ mRNA and protein levels and C/EBP α mRNA levels (Fig. 4, *A* and *D*). Additionally, we analyzed the effect of the different treatments on adipocyte expression of Fabp4/aP2, a gene well known to be regulated by Ppar γ . BC treatment reduced Fabp4/aP2 mRNA and protein expression 2.8- and 4.6-fold, respectively. Again, this effect was not observed in cells treated with BC in the presence of FHR or citral or upon treatment with either ROL or RA (Fig. 4, *D* and *E*). Thus, we conclude that endogenous RA derived from BC cleavage can decrease the expression of key lipogenic transcription factors in mature adipocytes.

Effects of BC in Mature Adipocytes Are Mediated by Rars—Our study showed that Bcmo1-dependent RA production can

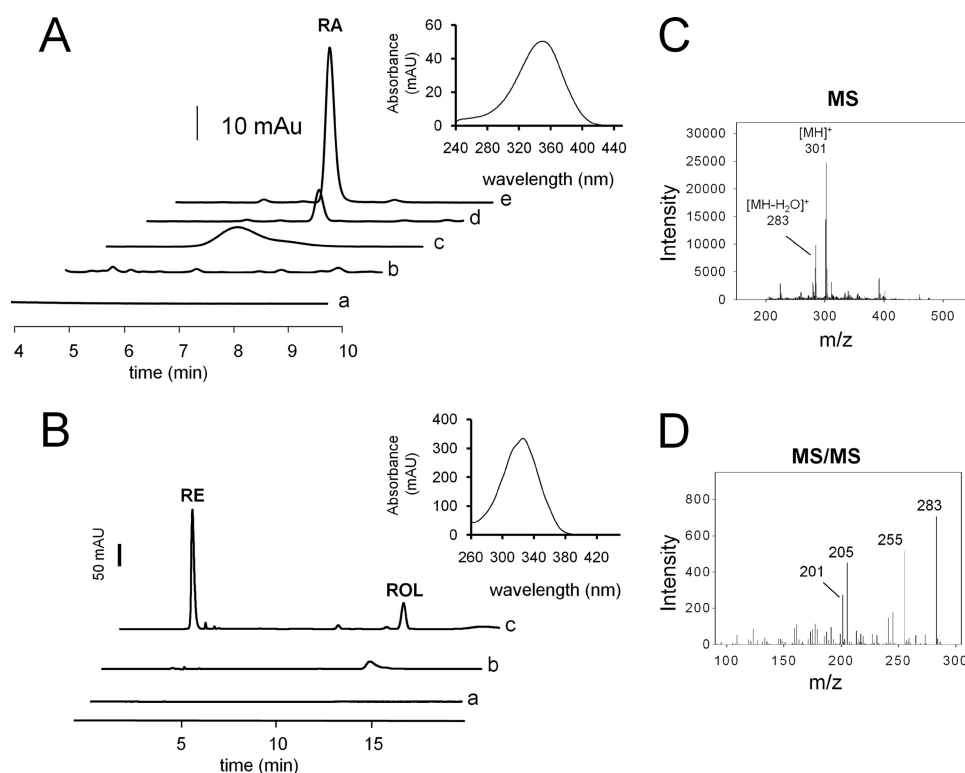


FIGURE 3. β,β -Carotene but not all-*trans*-retinol is converted to all-*trans*-retinoic acid in mature adipocytes. A, HPLC traces at 360 nm of polar retinoid extracts from 12.5 mg of untreated (a), ROL-treated (b), RA-treated (c), BC-treated (d), and BC-treated (e) mature NIH 3T3-L1 adipocytes. *Inset* shows the spectrum of RA peak of BC-treated mature NIH 3T3-L1 adipocytes. B, HPLC traces at 325 nm of nonpolar retinoid extracts from 12.5 mg of untreated (a), BC-treated (b), and ROL-treated (c) mature NIH 3T3-L1 adipocytes. The *inset* shows the spectrum of RE peak of ROL-treated mature NIH 3T3-L1 adipocytes. C, averaged MS spectrum collected for retinoic acid extracted from the peak indicated with RA in A. A prominent peak at $m/z = 301$ corresponds to molecular mass of retinoic acid ($[MH]^+$). Full mass spectrum showed ions that can be attributed to its dehydration product ($m/z = 283$). D, fragmentation pattern of a parent ion selected at $m/z = 301$ with characteristic peaks corresponding to loss of H_2O or COOH group ($m/z = 283$ and 255, respectively).

down-regulate *C/EBP α* and *Ppar γ* expression in mature NIH 3T3-L1 adipocytes. Inhibitory effects of RA on adipogenesis are largely mediated by RARs (7). To investigate whether the effects of BC-derived RA in mature adipocytes are RAR-dependent, we first analyzed *Cyp26a1* mRNA levels. *Cyp26a1* is an RA hydroxylase, and its mRNA expression is induced by RA in a strictly RAR-dependent manner (38, 39). In mature adipocytes treated with BC alone, *Cyp26a1* mRNA levels were 2.8-fold induced compared with control cells (supplemental Fig. S3A). This induction was not seen in mature adipocytes treated with either BC and FHR or BC and citral together. Additionally, ROL-treated cells failed to show induction of *Cyp26a1* mRNA expression (supplemental Fig. S3A). Thus, in agreement with RA production, BC treatment induced the expression of this RAR-responsive gene. To provide direct evidence that the effects of BC on adipocyte gene expression are mediated by Rars, we took advantage of the Rar pan-antagonist, LE450 (40). NIH 3T3-L1 adipocytes were pretreated with LE450 for 1 h prior to the addition of BC. After 24 h, we harvested cells and determined mRNA expression levels of *Cyp26a1*, *Ppar γ* , and *Fabp4/aP2*. Although BC treatment alone induced *Cyp26a1* and reduced *Ppar γ* and *Fabp4/aP2* mRNA levels, these effects were largely prevented by pretreatment with LE450 (supplemental Fig. S3, B–D). Additionally, treatment with LE450 prevented the effects of BC on the TG content of adipo-

cytes (supplemental Fig. S3E). Thus, we conclude that the effects of BC on mature adipocytes are RAR-dependent.

Dietary BC but Not ROL Decreases *Ppar γ* Expression—Our studies in cell culture indicated that BC plays an important role for retinoid signaling in mature adipocytes. Hence, one would expect that dietary BC but not preformed vitamin A exerts a similar role in animals. Therefore, we analyzed the effects of vitamin A deficiency as well as ROL and BC supplementation on adipose tissues of mice. *Lrat*^{−/−} mice cannot convert ROL to RE and lack retinoid stores in the liver (41). Therefore, these mice are highly susceptible to dietary vitamin A deficiency (41, 42). To induce vitamin A deficiency in these mice, we fed 8-week-old *Lrat*^{−/−} animals a diet either lacking any source of vitamin A ($n = 5$) or a vitamin A-sufficient diet ($n = 5$). After 3 weeks, we sacrificed the animals and isolated iWAT. As expected, HPLC analysis showed that retinoid levels were significantly reduced in iWAT of animals subjected to vitamin A deprivation (supplemental Fig. S4A). We next determined *Ppar γ* and

Fabp4/aP2 mRNA expression levels in the iWAT of these animals by qRT-PCR. Despite vitamin A deprivation, these mice exhibited no changes as compared with siblings maintained on a vitamin A-sufficient diet (Fig. 5A). Additionally, histology showed that adipocytes were comparable in size between the vitamin A-deficient and -sufficient animals (Fig. 5B and supplemental Fig. S4B). Thus, dietary restriction of preformed vitamin A had no effect on *Ppar γ* mRNA expression and activity in iWAT of mice.

We next gavaged vitamin A-deprived *Lrat*^{−/−} mice with the same amount of BC and ROL, respectively, or vehicle only. We then measured retinoid levels in iWAT of mice. Upon ROL treatment, retinoid levels significantly increased over levels in vehicle only-treated animals. An increase of retinoid levels was also found in animals gavaged with BC (Fig. 5C) but was less pronounced, indicating that ROL was more efficient than BC in replenishing vitamin A stores in iWAT. Trace amounts of BC (10.3 ± 4 pmol/g) became detectable in iWAT of *Lrat*^{−/−} mice gavaged with the provitamin but not in ROL and vehicle only-treated animals. Therefore, we next measured the effects of treatments on *Ppar γ* and *Cyp26a1* mRNA expression in iWAT (Fig. 5D). In ROL-treated animals, no changes of the mRNA levels of these genes became detectable as compared with vehicle only-treated controls. In contrast, in BC-treated animals, *Ppar γ* mRNA levels were 3-fold decreased, and *Cyp26a1*

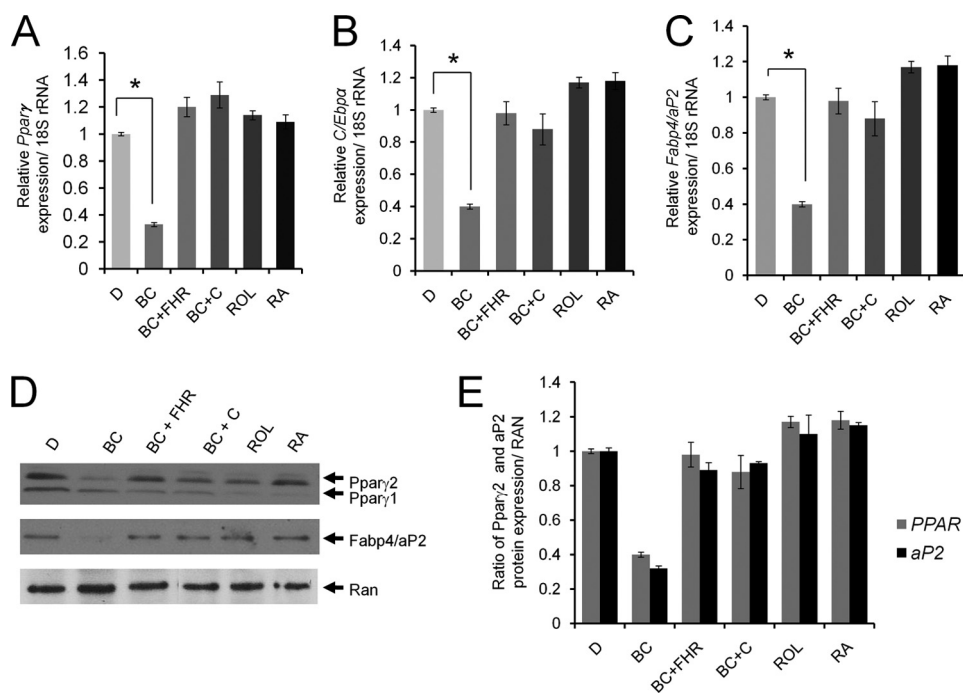


FIGURE 4. β,β -Carotene but not all-trans-retinol represses expression of key adipogenic markers. A–C, quantitative RT-PCR analysis of *Ppar γ* , *C/EBP α* , and *Fabp4/aP2* mRNA levels in mature NIH 3T3-L1 adipocytes, respectively, with and without treatments as indicated. D, representative *Ppar γ* and *Fabp4/aP2* immunoblots of mature NIH 3T3-L1 adipocytes with treatments as indicated. Ras-related nuclear protein (*Ran*) was used as a protein loading control. Error bars represent \pm S.D., $n = 3$ per condition. Two-tailed Student's *t* test; *, $p < 0.001$. Differentiated adipocytes (D, day 5). C, citral.

mRNA levels were 2.1-fold increased. Similar results were obtained after three consecutive treatments (24 h apart) with ROL and BC (Fig. 5E), indicating that BC but not ROL increased RA signaling and reduced *Ppar γ* in iWAT.

We also measured effects of different treatments on mRNA expression of key enzymes of retinoid metabolism in iWAT (Fig. 5, D and E). *Bcmo1* and retinal dehydrogenase 1 (*Raldh1*) mRNA levels were 4- and 2.1-fold increased, respectively, after a single treatment with BC as compared with vehicle only-treated animals. *Raldh1* acts downstream of *Bcmo1* and converts the BC cleavage product RAL to RA. In contrast, *Adh1* mRNA expression was 4-fold decreased under this condition. This alcohol dehydrogenase catalyzes RAL to ROL conversion. No changes in the mRNA expression of these genes were observed in ROL-treated animals. Thus, BC induced mRNA expression of genes encoding key enzymes for RA production in iWAT, including *Bcmo1* and *Raldh1*, and repressed expression of the enzyme for RAL to ROL conversion.

DISCUSSION

Here, we showed in cell culture and mouse models that BC is the physiological precursor for RA production in adipocytes. RA production from BC strictly depended on the activity of *Bcmo1* that was expressed as a *Ppar γ* -induced gene during adipogenesis. BC but not ROL reduced *Ppar γ* expression and lipid content of mature adipocytes. These findings provide evidence that *Bcmo1* plays a critical role for the cross-talk between *Ppar γ* and *Rar* signaling pathways and implicates BC as an important dietary regulator of fat storage capacities of adipocytes.

BC Is a Physiological Precursor for RA Production in Adipocytes—

Upon cloning *Bcmo1*, a surprising result was that steady-state mRNA levels of the vitamin A-forming enzyme were relatively high in peripheral nondigestive tissues, including adipocytes (20–22). These findings indicate that besides intestinal conversion of BC and transport of vitamin A, a tissue-specific conversion of the provitamin may influence retinoid-dependent physiological processes. *Bcmo1*-deficient mice accumulate BC in various tissues, including adipocytes, indicating that the BC substrate is well distributed within the body (26). Promoter analysis revealed that *Bcmo1* is a *Ppar*-induced gene that contains a peroxisome proliferator-binding responsive element that binds *Ppar γ* /*Rxr* heterodimers (23). In fact, we showed here that *Bcmo1* expression increased during adipogenesis of NIH 3T3-L1 cells both at the mRNA and protein levels. Treatment of mature NIH 3T3-L1 adipocytes with BC resulted in RA production. RA production was significantly reduced in the presence of FHR that inhibited enzymatic activity of recombinant *Bcmo1*. In contrast, treatment of mature NIH 3T3-L1 adipocytes with preformed vitamin A resulted in RE but not RA production. In conformity with the cell culture study, gavage of BC but not ROL induced expression of the classical RA-induced target gene *Cyp26a1* in the iWAT of vitamin A-deficient mice.

This critical role of BC for RA metabolism might be explained by specific biochemical characteristics of adipocyte. Previous studies have revealed that enzymatic activity of *Bcmo1* is stimulated in the presence of cellular retinol-binding protein 1 (*Crpb1*) (27). *Crpb1* can bind RAL, the BC cleavage product, and is expressed in various tissues, including adipocytes (43). In the liver, *Crpb1* stimulates RE formation, the storage form of vitamin A, from *Crpb1*-bound retinoids in a *LRAT*-dependent manner (44). Adipocytes express different acyltransferases than *Lrat* for RE formation (41). Additionally, the expression of the RAL to ROL-converting enzyme *Adh1* is decreased during adipogenesis (18). Additionally, our study showed that BC treatment decreased *Adh1* mRNA expression, whereas it induced *Bcmo1* and *Raldh1* mRNA expression in iWAT. Thus, reduced expression of *Adh1* and, on the other hand, induced expression of *Bcmo1* and *Raldh1* (this study and see Ref. 18) likely explain why the primary BC cleavage product, RAL, is predominantly metabolized into RA in adipocytes.

BC Decreases *Ppar γ* Signaling and Lipid Storage Capacity of Adipocytes—Previous analyses of *Bcmo1* knock-out mice have already indicated a specific role of *Bcmo1* for retinoid metabolism in adipose tissues. *Bcmo1*^{−/−} mice show increased expres-

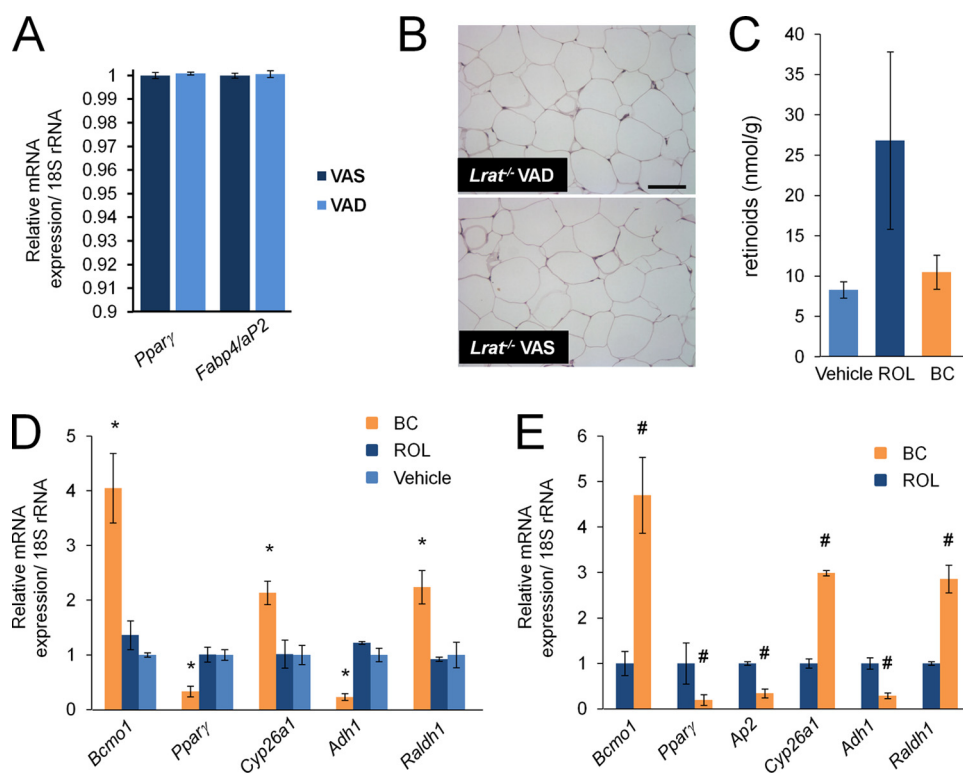


FIGURE 5. Effects of β , β -carotene and vitamin A on adipose tissue of *Lrat*^{-/-} mice. A and B, *Lrat*^{-/-} mice ($n = 5$ per group) were maintained either on a VAD or a vitamin A-sufficient diet (VAS). A, relative mRNA expression of key adipogenic genes in iWAT of *Lrat*^{-/-} mice provided with diets indicated. B, representative images of H&E-stained sections of iWAT from *Lrat*^{-/-} mice provided with diets as indicated. The scale bar represents 200 μ m. C and D, *Lrat*^{-/-} mice were maintained for 10 days on a vitamin A-deficient diet. The animals ($n = 3$ per condition) were then gavaged with 0.5 mg of BC or ROL dissolved in 100 μ l of corn oil or vehicle only. 24 h after gavage, animals were sacrificed. Retinoid levels (retinyl esters and all-*trans*-retinol) (C) and mRNA levels of *Bcmo1*, *Ppar γ* , *Cyp26a1*, *Adh1*, and *Raldh1* (D) were quantified in iWAT of animals. In the experiments, error bars represent \pm S.D., $n = 3$ per group. Two-tailed Student's *t* test; *, $p < 0.05$ as compared with vehicle only-treated animals. E, *Lrat*^{-/-} mice were maintained for 10 days on a vitamin A-deficient diet. The animals ($n = 5$ per condition) were then gavaged with 0.5 mg of BC or ROL dissolved in 100 μ l of corn oil. Gavage was performed three times in 24-h intervals. 24 h after the last gavage, animals were sacrificed, and mRNA levels of *Bcmo1*, *Ppar γ* , *Fabp4/aP2*, *Cyp26a1*, *Adh1*, and *Raldh1* were determined in iWAT. In the experiments, error bars represent \pm S.D.; $n = 5$ per group. Two-tailed Student's *t* test; #, $p < 0.05$ as compared with all-*trans*-retinol-treated animals. VAS, vitamin A-sufficient diet.

sion of *Ppar γ* -induced genes in iWAT and are more susceptible to diet-induced obesity (26). Our current analysis provided a molecular and mechanistic explanation for this phenotype by showing that *Bcmo1* plays an important role for RA production in adipocytes. RA is the ligand of Rars that act in conjunction with Rxrs. During preadipocyte to adipocyte conversion, liganded Rar interferes with transcriptional activation of *Ppar γ* by *C/Ebbs*, possibly by competing for common and limiting cofactors (7). Importantly, RA can exert this effect when the transcription of *Ppar γ* has already been induced during adipocyte differentiation (35). We found that BC-derived RA reduced the expression of the key lipogenic transcription factors *Ppar γ* and *C/Ebpa* in mature 3T3-L1 adipocytes. The decrease in the expression of these transcription factors was accompanied by a down-regulation of *Fabp4/aP2* expression and a reduction in the TG content of cells. These effects of BC on mature adipocytes was prevented by the Rar pan-antagonist LE450, pointing to a critical role for liganded Rars in mediating it. Thus, in mature adipocytes RA derived from BC conversion may decrease *Ppar γ* expression by a related mechanism as during preadipocyte to adipocyte conversion. Such a reduction of

Ppar γ expression and signaling has been shown to promote fat mobilization in adipocytes (45). Additionally, RA has been implicated to increase the capacity for oxidative metabolism and to induce lipolysis of stored TG in adipocytes (8, 12). These effects are explained, at least in part, by direct RA-dependent activation of Rar-regulated target genes. Both the RA-dependent reduction of *Ppar γ* expression and induction of oxidative metabolism and lipolysis result in a reduced capacity of fat storage in adipocytes. Conversely, the storage capacity for fat is increased in *Bcmo1*-deficient adipocytes as evidenced by analysis in *Bcmo1*^{-/-} mice (26).

In conclusion, we provided experimental evidence that *Bcmo1* expression is induced by *Ppar γ* during adipogenesis. In mature adipocytes, BC was converted to RA and decreased *Ppar γ* signaling in a Rar-dependent manner. This cross-talk between these key signaling pathways may integrate important information about the energy and vitamin A status of the diet. Blood levels of BC are highly variable and responsive to diet. In contrast, blood levels of ROL are closely controlled and would not provide information about the vitamin A status of the diet. One might speculate that a diet rich in BC and fat directs this

process toward energy expenditure, including reproduction, a process in which BC-derived retinoids play a pivotal role (47). In the absence of BC, adipocytes increasingly store energy in the form of fat. In humans, circulating BC levels are inversely correlated with risk of type 2 diabetes, a pathology associated with obesity (36, 48–50). Additionally, reduced plasma levels of carotenoids, including BC, are commonly found in obese children (46). Thus, the complex role of BC in adipocyte biology in health and disease deserves further research.

Acknowledgments—We thank Catherine Doller for performing the H&E staining on the mouse adipose tissues and Dr. Scott Howell for morphometric analysis (Department of Pathology, Case Western Reserve University, Cleveland, OH).

REFERENCES

- Bonet, M. L., Ribot, J., Felipe, F., and Palou, A. (2003) *Cell. Mol. Life Sci.* **60**, 1311–1321
- Ziouzenkova, O., and Plutzky, J. (2008) *FEBS Lett.* **582**, 32–38
- Kawada, T., Kamei, Y., and Sugimoto, E. (1996) *Int. J. Obes. Relat. Metab. Disord.* **20**, S52–S57

4. Ribot, J., Felipe, F., Bonet, M. L., and Palou, A. (2001) *Obes. Res.* **9**, 500–509
5. Gorocica-Buenfil, M. A., Fluharty, F. L., Bohn, T., Schwartz, S. J., and Loerch, S. C. (2007) *J. Anim. Sci.* **85**, 3355–3366
6. Kuri-Harcuch, W. (1982) *Differentiation* **23**, 164–169
7. Schwarz, E. J., Reginato, M. J., Shao, D., Krakow, S. L., and Lazar, M. A. (1997) *Mol. Cell. Biol.* **17**, 1552–1561
8. Berry, D. C., and Noy, N. (2009) *Mol. Cell. Biol.* **29**, 3286–3296
9. Alvarez, R., de Andrés, J., Yubero, P., Viñas, O., Mampel, T., Iglesias, R., Giralt, M., and Villarroya, F. (1995) *J. Biol. Chem.* **270**, 5666–5673
10. Puigserver, P., Vázquez, F., Bonet, M. L., Picó, C., and Palou, A. (1996) *Biochem. J.* **317**, 827–833
11. Mercader, J., Ribot, J., Murano, I., Felipe, F., Cinti, S., Bonet, M. L., and Palou, A. (2006) *Endocrinology* **147**, 5325–5332
12. Mercader, J., Madsen, L., Felipe, F., Palou, A., Kristiansen, K., and Bonet, M. L. (2007) *Cell. Physiol. Biochem.* **20**, 1061–1072
13. Hollung, K., Rise, C. P., Drevon, C. A., and Reseland, J. E. (2004) *J. Cell. Biochem.* **92**, 307–315
14. Felipe, F., Bonet, M. L., Ribot, J., and Palou, A. (2004) *Diabetes* **53**, 882–889
15. Felipe, F., Mercader, J., Ribot, J., Palou, A., and Bonet, M. L. (2005) *Biochim. Biophys. Acta* **1740**, 258–265
16. Mercader, J., Granados, N., Bonet, M. L., and Palou, A. (2008) *Cell. Physiol. Biochem.* **22**, 363–372
17. Petkovich, M., Brand, N. J., Krust, A., and Chambon, P. (1987) *Nature* **330**, 444–450
18. Ziouzenkova, O., Orasanu, G., Sharlach, M., Akiyama, T. E., Berger, J. P., Viereck, J., Hamilton, J. A., Tang, G., Dolnikowski, G. G., Vogel, S., Duester, G., and Plutzky, J. (2007) *Nat. Med.* **13**, 695–702
19. Felipe, F., Bonet, M. L., Ribot, J., and Palou, A. (2003) *Int. J. Obes. Relat. Metab. Disord.* **27**, 60–69
20. Paik, J., During, A., Harrison, E. H., Mendelsohn, C. L., Lai, K., and Blaner, W. S. (2001) *J. Biol. Chem.* **276**, 32160–32168
21. Redmond, T. M., Gentleman, S., Duncan, T., Yu, S., Wiggert, B., Gantt, E., and Cunningham, F. X., Jr. (2001) *J. Biol. Chem.* **276**, 6560–6565
22. Kiefer, C., Hessel, S., Lampert, J. M., Vogt, K., Lederer, M. O., Breithaupt, D. E., and von Lintig, J. (2001) *J. Biol. Chem.* **276**, 14110–14116
23. Boulanger, A., McLemore, P., Copeland, N. G., Gilbert, D. J., Jenkins, N. A., Yu, S. S., Gentleman, S., and Redmond, T. M. (2003) *FASEB J.* **17**, 1304–1306
24. Gong, X., Tsai, S. W., Yan, B., and Rubin, L. P. (2006) *BMC Mol. Biol.* **7**, 7
25. Lefterova, M. I., and Lazar, M. A. (2009) *Trends Endocrinol. Metab.* **20**, 107–114
26. Hessel, S., Eichinger, A., Isken, A., Amengual, J., Hunzelmann, S., Hoeller, U., Elste, V., Hunziker, W., Goralczyk, R., Oberhauser, V., von Lintig, J., and Wyss, A. (2007) *J. Biol. Chem.* **282**, 33553–33561
27. Fierce, Y., de Moraes Vieira, M., Piantadosi, R., Wyss, A., Blaner, W. S., and Paik, J. (2008) *Arch. Biochem. Biophys.* **472**, 126–138
28. Lobo, G., Hessel, S., Eichinger, A., Noy, N., Moise, A. R., Wyss, A., Palczewski, K., and von Lintig, J. (2010) *FASEB J.* **24**, 1656–1666
29. von Lintig, J., and Vogt, K. (2000) *J. Biol. Chem.* **275**, 11915–11920
30. Isken, A., Holzschuh, J., Lampert, J. M., Fischer, L., Oberhauser, V., Palczewski, K., and von Lintig, J. (2007) *J. Biol. Chem.* **282**, 1144–1151
31. Oberhauser, V., Voolstra, O., Bangert, A., von Lintig, J., and Vogt, K. (2008) *Proc. Natl. Acad. Sci. U.S.A.* **105**, 19000–19005
32. Golczak, M., Kuska, V., Maeda, T., Moise, A. R., and Palczewski, K. (2005) *Proc. Natl. Acad. Sci. U.S.A.* **102**, 8162–8167
33. Golczak, M., Imanishi, Y., Kuska, V., Maeda, T., Kubota, R., and Palczewski, K. (2005) *J. Biol. Chem.* **280**, 42263–42273
34. Sergeant, M. J., Li, J. J., Fox, C., Brookbank, N., Rea, D., Bugg, T. D., and Thompson, A. J. (2009) *J. Biol. Chem.* **284**, 5257–5264
35. Xue, J. C., Schwarz, E. J., Chawla, A., and Lazar, M. A. (1996) *Mol. Cell. Biol.* **16**, 1567–1575
36. Ylönen, K., Alftan, G., Groop, L., Saloranta, C., Aro, A., and Virtanen, S. M. (2003) *Am. J. Clin. Nutr.* **77**, 1434–1441
37. Noy, N. (1992) *Biochim. Biophys. Acta* **1106**, 151–158
38. Abu-Abed, S., Dollé, P., Metzger, D., Beckett, B., Chambon, P., and Petkovich, M. (2001) *Genes Dev.* **15**, 226–240
39. Emoto, Y., Wada, H., Okamoto, H., Kudo, A., and Imai, Y. (2005) *Dev. Biol.* **278**, 415–427
40. Kagechika, H., Kawachi, E., Fukasawa, H., Saito, G., Iwanami, N., Umeyama, H., Hashimoto, Y., and Shudo, K. (1997) *Biochem. Biophys. Res. Commun.* **231**, 243–248
41. O'Byrne, S. M., Wongsiriroj, N., Libien, J., Vogel, S., Goldberg, I. J., Baehr, W., Palczewski, K., and Blaner, W. S. (2005) *J. Biol. Chem.* **280**, 35647–35657
42. Liu, L., and Gudas, L. J. (2005) *J. Biol. Chem.* **280**, 40226–40234
43. Zovich, D. C., Orologa, A., Okuno, M., Kong, L. W., Talmage, D. A., Piantadosi, R., Goodman, D. S., and Blaner, W. S. (1992) *J. Biol. Chem.* **267**, 13884–13889
44. Molotkov, A., Ghyselinck, N. B., Chambon, P., and Duester, G. (2004) *Biochem. J.* **383**, 295–302
45. Picard, F., Kurtev, M., Chung, N., Topark-Ngarm, A., Senawong, T., Machado De Oliveira, R., Leid, M., McBurney, M. W., and Guarente, L. (2004) *Nature* **429**, 771–776
46. Burrows, T. L., Warren, J. M., Colyvas, K., Garg, M. L., and Collins, C. E. (2009) *Obesity* **17**, 162–168
47. Ross, S. A., McCaffery, P. J., Drager, U. C., and De Luca, L. M. (2000) *Physiol. Rev.* **80**, 1021–1054
48. Coyne, T., Ibiebele, T. I., Baade, P. D., Dobson, A., McClintock, C., Dunn, S., Leonard, D., and Shaw, J. (2005) *Am. J. Clin. Nutr.* **82**, 685–693
49. Ford, E. S., Will, J. C., Bowman, B. A., and Narayan, K. M. (1999) *Am. J. Epidemiol.* **149**, 168–176
50. Ramakrishna, V., and Jaikhan, R. (2008) *Acta Diabetol.* **45**, 41–46